THE JOURNAL OF PHYSICAL CHEMISTRY C
A JOURNAL OF THE AMERICAN CHEMICAL SOCIETY

pubs.acs.org/JPCC

Article

Triplet Exciton Diffusion and Quenching in Matrix-Free Solid Photon Upconversion Films

Steponas Raišys, Ona Adomėnienė, Povilas Adomėnas, Alexander Rudnick, Anna Köhler, and Karolis Kazlauskas*

Cite This: J. Phys. Chem. C 2021, 125, 3764–3775

Read Online

ACCESS | Metrics & More | Article Recommendations | Supporting Information

ABSTRACT: Efficient triplet exciton hopping (diffusion) in amorphous solid films is essential for triplet−triplet annihilation (TTA) and TTA-mediated photon upconversion (UC) at low excitation power densities. However, enhanced triplet diffusion, particularly in high-emitter-content UC films, also facilitates their trapping and quenching at nonradiative decay sites, thus deteriorating UC efficiency. In this work, triplet exciton diffusion and quenching are studied in matrix-free solid UC films based on two novel bisfluorene-anthracene (BFA) emitters, i.e., one with methyl substitution (BFA-Me) and the other with a phenyl substitution (BFA-Ph), and a standard platinum octaethylporphyrin (PtOEP) sensitizer. By analyzing temperature-dependent TTA-UC dynamics and accounting for various singlet exciton-related processes, we are able to discern triplet exciton quenching occurring explicitly in the emitter and show that it is one of the dominating mechanisms impeding the UC performance of BFA/PtOEP films, particularly at elevated temperatures. Regardless of the lower density of quenchers present in the BFA-Ph film, twice as large triplet diffusivity estimated in this film ($D = (2.13 \pm 0.64) \times 10^{-9}$ cm^2·s^{-1}) at room temperature as compared to that in the BFA-Me film caused more rapid triplet quenching. This resulted in the shifting of the optimal UC performance of BFA-Ph to lower temperatures ($T = 160$ K) with respect to that of BFA-Me ($T = 220$ K). To obtain a high UC quantum yield, which for these materials can be estimated to reach >5% at room temperature and above, the excessive diffusion to the remaining quenching sites needs to be suppressed, e.g., by increasing the intermolecular distance through side groups.

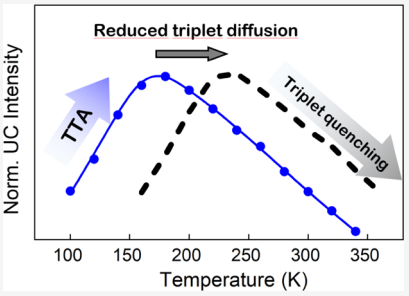

INTRODUCTION

Triplet-mediated photon upconversion (UC) is a noncoherent process that involves the conversion of two lower-energy photons into a single photon of higher energy and has been employed in a vast variety of important technological applications ranging from photocatalysis[1] to bioimaging[2] and photovoltaics.[3−5] Consisting of several subsequent events, sensitized UC is initiated in the sensitizer, where incident photons are absorbed forming excited singlet states, which then rapidly convert into triplets through an intersystem crossing (ISC).[6,7] The process is followed by the so-called triplet sensitization, i.e., triplet energy transfer (TET) to the emitter forming long-lived triplet states, where triplet exciton concentration develops until triplet−triplet annihilation (TTA) becomes probable. Eventually, TTA populates singlet excited states of the emitter, resulting in UC photon emission (the detailed TTA-UC scheme is provided in Scheme 1).

More energetic photons produced via the UC scheme were shown to be able, for example, to drive photocatalytic reactions such as water splitting for hydrogen generation,[8,9] trigger drug delivery,[10] enhance photoconversion efficiency of solar cells,[4,11] etc.[12−14] Undoubtedly, the big advantage of the UC process, originating from the long-lived intermediate triplet states involved, is the possibility to be driven by incoherent

Scheme 1. TTA-UC Energy Scheme[a]

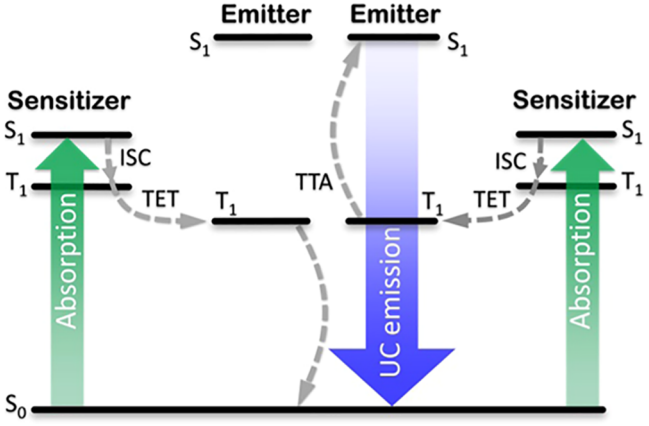

[a]ISC: intersystem crossing, TET: triplet energy transfer, TTA: triplet−triplet annihilation, and UC: upconversion.

Received: December 10, 2020
Revised: January 28, 2021
Published: February 11, 2021

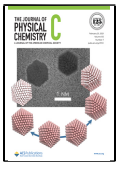

light and at low power densities on the order of ~mW·cm^{-2} (~1 sun).[15] Since the practical TTA-UC applications depend crucially on the UC quantum yield (Φ_{UC}), much effort is currently being devoted toward optimization of Φ_{UC}.

To obtain TTA-UC, two triplet excitons need to meet during their lifetime. Therefore, the TTA-UC performance relies heavily on the triplet energy transfer, which is a Dexter-type process and requires sufficient wavefunction overlap of the neighboring molecules.[16] In the liquid state, short-range exchange interactions are accomplished through molecular diffusion. Presently, the highest Φ_{UC} of up to 38% is achieved in solutions/liquids.[17−19] Note that one photon at most can be produced per two absorbed ones during the TTA-UC process, implying a maximum Φ_{UC} of 50%.[18,20] This definition was used throughout our work. For the majority of practical UC applications, however, solid systems are preferred. In rigid UC films with molecule positions fixed, the encounter of two triplet excitons can only occur via triplet exciton diffusion, e.g., exciton hopping in disordered media. To avoid the formation of poorly emissive excimers or aggregate species that may act as nonradiative decay sites as well as to suppress exciton transfer to other defect sites such as chemical defects and oxygen- or water-related complexes,[21] it is a common practice to use a low concentration of sensitizers and dyes in an electronically inert matrix.[22,23] One finds that in many of the rigid, yet amorphous solid systems, Φ_{UC} is about 1 order of magnitude lower than in liquid systems.[24−31] This is primarily attributed to severely limited triplet diffusion in the rigid films.[22,32] The most common approach to circumvent the issue of insufficient triplet exciton diffusion is the so-called "soft" matrix approach, which relies on using low glass transition temperature (T_g) matrixes to accommodate sensitizer and emitter pairs. The soft matrix is considered to allow for a high degree of rotational and translational motion of excited molecular species, thereby facilitating triplet diffusion and TTA. Indeed, for soft "solid systems" such as elastomers,[33,34] gels,[35,36] or nano/microparticles,[37−40] Φ_{UC} values of about 10 ± 5% are reported, which are greatly improved with respect to the values obtained in rigid hosts. A nanofibrous crystalline system was reported by Ogawa et al. to give Φ_{UC} = 4.5% (when using 50% for the maximum value).[41] While the glass transition temperature T_g is not reported for this system, its chemical structure is akin to liquid crystals,[42] so that an overall soft film at room temperature can be expected.

The usage of soft, low T_g (i.e., T_g near or below room temperature) matrices is a problem for practical applications such as solar cells. Such devices can be exposed to higher operating temperatures where the device becomes liquid-like. Materials with higher T_g would be of advantage here. Previous work using poly(methyl methacrylate) (PMMA) as a matrix with a T_g of around 100 °C is encouraging. Using heavily doped PMMA films (15−40 wt % emitter content in the PMMA host) for enhanced triplet diffusion, one of the highest Φ_{UC} values (2.7%) in rigid sensitized UC polymers was achieved.[27,30] A promising approach to further facilitate triplet diffusion seems to be to omit the matrix and focus on neat, matrix-free films.[31,43,44] This approach, however, is anticipated to face additional challenges related to diffusion-enhanced triplet trapping and quenching at nonradiative decay sites.[27,45,46] Note that mostly the triplet quenching in sensitizer aggregates is considered as these are encountered at concentrations of 2−6 wt % typically used in solid UC films.[45,47,48] The quenching in the sensitizer can be relatively simply probed via phosphorescence signal, whereas probing triplet quenching in the emitter is more difficult since TTA emitters (anthracenes, tetracenes, and other acenes) usually exhibit almost undetectable phosphorescence because of the efficient TTA and/or nonradiative triplet decay in the neat films. Hence, the impact of diffusion-facilitated triplet quenching, particularly in the emitter species, is frequently overlooked, although it can drastically reduce Φ_{UC}, primarily in high-emitter-content UC films. The issue of triplet quenching, however, was touched upon in the previous reports by Karpicz et al.[48] and Goudarzi et al.,[45,46] where temperature-dependent photon upconversion in matrix-free solid 9,10-diphenylanthracene (DPA)/platinum octaethylporphyrin (PtOEP) systems was studied. We note that these systems exhibited poor UC performance, as they suffered from immense DPA as well as PtOEP aggregation and the associated exciton quenching, resulting in 10−100 times stronger PtOEP phosphorescence as compared to UC intensity. Moreover, we stress that in the previous reports, the triplet-related processes in the temperature dynamics of TTA-UC were not decoupled from those associated with singlets and thus have not been explicitly studied so far.

To this end, in the current contribution, we address triplet exciton quenching in the emitter species by utilizing the delayed UC signal as a probe of the triplet population. The quenching is investigated in matrix-free (bicomponent) amorphous UC systems based on carefully designed bisfluorene-anthracene (BFA) emitters coupled with a standard platinum octaethylporphyrin (PtOEP) sensitizer. The exceptionally low sensitizer concentrations employed (0.03 wt %) are intended to prevent, first, detrimental sensitizer aggregation and associated triplet quenching and, second, parasitic energy back transfer from the emitter to the sensitizer. The BFA emitters were developed with an intention to outperform the state-of-the-art 9,10-diphenylanthracene (DPA) emitter in terms of (i) ease of processability into UC films, (ii) reduced aggregation eliminating the need to use a matrix, and (iii) increased overall UC performance. The new BFA emitters feature a non-symmetrically substituted anthracene core and twisted peripheral dihexyl-fluorenyl moieties, which ensure rigid glassy UC films as well as low concentration quenching of emission. By monitoring temperature-dependent TTA-UC dynamics and accounting for various temperature-induced processes such as triplet transfer from PtOEP to BFA as well as the processes associated with singlets, namely, changes in PtOEP absorption and FL quenching in BFA, the triplet diffusion-facilitated processes, i.e., TTA and nonradiative triplet quenching in the BFA emitters were discerned. The revealed differences in the triplet quenching of BFA emitters causing maximal UC intensity of BFA/PtOEP films to occur at different temperatures were explained by the essential role of triplet exciton diffusion, which was evaluated in these films using the time-resolved emission bulk-quenching technique.[49]

EXPERIMENTAL METHODS

Materials and Synthesis. Chemicals including PtOEP, PMMA, and phenyl-C_{61}-butyric acid methyl ester (PCBM) were purchased from Sigma-Aldrich and were used as received. Synthesis and identification of the bisfluorene-anthracene compounds BFA-Me and BFA-Ph (Figure 1a) are provided in the Supporting Information (Schemes S1−S3, Figures S1

https://dx.doi.org/10.1021/acs.jpcc.0c11048
J. Phys. Chem. C 2021, 125, 3764−3775

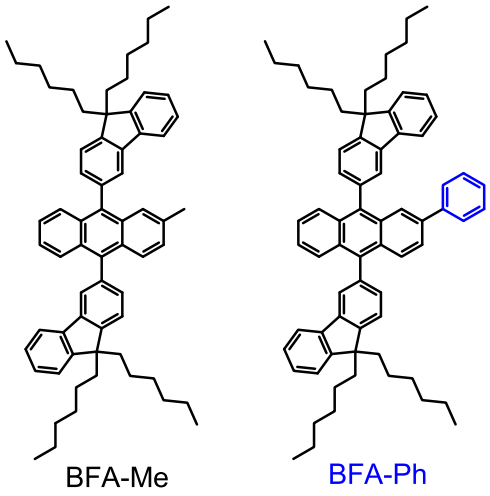

Figure 1. Chemical structures of bisfluorene-anthracene compounds BFA-Me and BFA-Ph.

and S2). The two compounds differ by the methyl or phenyl side group that is attached to the anthracene core.

Preparation of the Upconverting Films. Upconverting BFA/PtOEP films were prepared in a nitrogen-filled glovebox with O_2 and H_2O concentrations below 0.1 ppm. Chloroform solutions of each BFA compound (20 mg·mL^{-1}) and PtOEP (6 μg·mL^{-1}) were drop-casted (in an amount of 50 μL) on precleaned microscope glass slides at 70 °C and left to dry for 15 min to result in BFA films doped with PtOEP at a concentration of 0.03 wt %. Later, the BFA/PtOEP samples were annealed at 140 °C for 3 min and then rapidly cooled to below T_g with extra cover glass slides placed on top to form smooth 8 ± 1 μm thick films.

For evaluation of triplet exciton diffusion, varying amounts of PCBM quencher were additionally introduced into the chloroform solutions to give a final concentration of 0−0.7 wt % of PCBM in the BFA/PtOEP films. The prepared films were encapsulated inside a glovebox using epoxy resin prior to conducting different types of photophysical measurements at ambient conditions.

An additional set of samples, i.e., neat BFA films and PtOEP-doped PMMA films (c_{PtOEP} = 0.03 wt %) were prepared and encapsulated inside the glovebox in a similar manner.

Photophysical Measurements. Absorption spectra of the films were recorded using a UV−vis−NIR spectrophotometer Lambda 950 (PerkinElmer). Fluorescence of the samples was excited at 370 nm using a 150 W xenon arc lamp (LOT-Oriel) coupled to a single monochromator 9030 (Sciencetech), whereas UC emission was induced by exciting at 532 nm using a 200 mW continuous-wave semiconductor laser diode (APT lighting). Emission was measured employing a back-thinned CCD spectrometer PMA-11 (Hamamatsu). The fluorescence and UC emission quantum yield were estimated by utilizing a 6″ integrating sphere (Sphere Optics) coupled to the same CCD spectrometer via an optical fiber.

Delayed UC fluorescence and phosphorescence were recorded utilizing a time-gated intensified CCD camera New iStar DH334T (Andor) coupled to a spectrograph Oriel MS257 (Newport). In these experiments, a frequency-doubled pulsed Nd3+:YAG laser (Innolas) (wavelength: 532 nm, pulse duration: 7 ns, and repetition rate: 20 Hz) served as an excitation source. The temperature-dependent emission measurements were performed with the samples mounted in a continuous flow helium cryostat OptistatCF (Oxford Instruments) under a helium atmosphere, while the temperature was controlled with an intelligent temperature controller ITC-502 (Oxford). Differential scanning calorimetry (DSC) measurements were carried out using a DSC 1 thermal analyzer (Mettler Toledo) at a heating rate of 10 °C·min^{-1} under nitrogen flow. The film thickness was determined by measuring the surface profile of the scratched area with a Dimension Icon atomic force microscope (AFM, Bruker). Glass transition temperatures of BFA neat and 0.03 wt % PtOEP-doped BFA films were estimated using AFM-based thermal analysis at the nanoscale level (Dimension Icon, Bruker).

RESULTS AND DISCUSSION

Photophysical Properties. The structures of rationally designed bisfluorene-anthracene (BFA) compounds used as emitters in solid UC films are displayed in Figure 1. Synthesis and identification of the BFA compounds are provided in the Supporting Information (Schemes S1−S3, Figures S1 and S2). Both compounds are based on the anthracene core symmetrically substituted with dihexyl-fluorenyl groups at the 9- and 10-positions and non-symmetrically substituted with methyl (BFA-Me) or phenyl (BFA-Ph) group at the 2-position. The choice to use the anthracene core was based on its inherent capability to express the efficient TTA required for the emitters/annihilators employed in UC.[22,50,51] Highly twisted peripheral fluorenyl groups (dihedral angles with the core are close to 90°) as well as long alkyl moieties ensured good solubility in common organic solvents and prevented close $\pi-\pi$ stacking, thus rendering amorphous morphology of the BFA films. Glassy state formation with T_g values of about 55 and 65 °C for compounds BFA-Me and BFA-Ph, respectively, was determined from DSC measurements (Figure S3 in the Supporting Information). Similar T_g values were obtained by performing nanoscale thermal analysis of BFA films at different spots using a dedicated AFM probe (Figure S4 in the Supporting Information). PtOEP-doped BFA films identical to those used for UC measurements exhibited slightly larger T_g values of up to 74 ± 4 °C (Figure S5 in the Supporting Information), signifying that at room temperature, the studied UC films are rigid and TTA can only occur via exciton hopping (diffusion). Additionally, the twisted geometry of the BFA along with the branchy alkyl chains benefited from low concentration quenching of emission, resulting in high fluorescence quantum yield (up to 71%) of the neat BFA films. The high fluorescence yield of the emitters is a prerequisite for high Φ_{UC}. A comparison of the solid-state emission spectra, fluorescence quantum yields (Φ_{FL}), and lifetimes with those in dilute solutions for the BFA compounds is presented in Figure S7 in the Supporting Information.

Fluorescence spectra of the neat BFA films are shown in Figure 2, where they are overlapped with the absorption spectrum of the PtOEP sensitizer. BFA-Me has an emission band peaked at a similar wavelength as that of the widely used 9,10-diphenylanthracene emitter (~440 nm),[30] whereas the emission of BFA-Ph featuring a phenyl-substituted anthracene core is redshifted by ~20 nm (~0.12 eV) as a result of slightly enhanced conjugation. It is also evident that the emission of BFA falls between the higher-energy Soret band and the lower-energy Q band of PtOEP, indicating relatively low reabsorption, i.e., low energy back transfer to the sensitizer.

https://dx.doi.org/10.1021/acs.jpcc.0c11048
J. Phys. Chem. C 2021, 125, 3764−3775

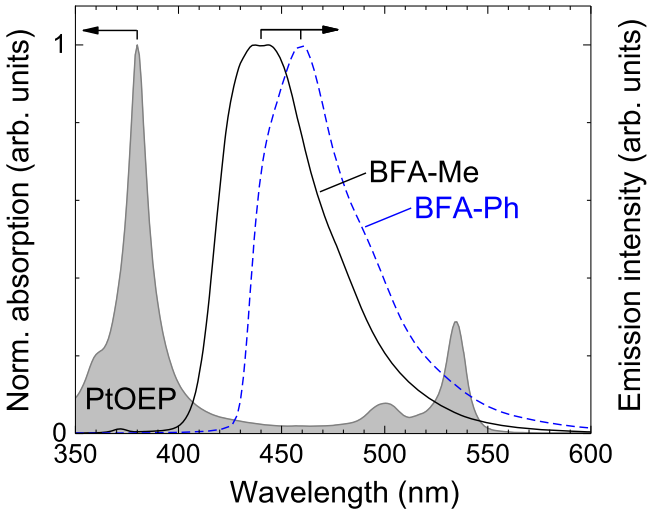

Figure 2. Normalized absorption and emission spectra of PtOEP in PMMA (c_{PtOEP} = 0.03 wt %), BFA-Me, and BFA-Ph neat films. Emission excitation wavelength: 370 nm.

PtOEP concentration in the studied UC films based on the BFA/PtOEP system was fixed at 0.03 wt %, which was found to be close to optimal (Figure S8 in the Supporting Information). Φ_{FL} values of these UC films (BFA-Me/PtOEP and BFA-Ph/PtOEP) were determined to be 42 and 36%, respectively. An almost 2-fold lower Φ_{FL} value of the BFA/PtOEP films as compared to that of the neat BFA films is attributed to the energy transfer from BFA to PtOEP despite the very low sensitizer concentration utilized. This occurs due to some residual overlap of emitter fluorescence and sensitizer absorption (Figure 2) and has been previously demonstrated to be a serious issue in high-emitter-content UC systems.[30]

Triplet States of BFA Emitters. Triplet state energies of BFA emitters employed in the UC scheme were identified by measuring the low-temperature phosphorescence of PtOEP-sensitized BFA films excited at 532 nm (Figure 3a). Figure 3a also displays TTA-UC emission measured at 5 K. Typically, a phosphorescence spectrum resembles a fluorescence spectrum; however, in the case of thick BFA films, the intensity of the zeroth vibronic peak of UC emission was diminished due to the reabsorption effect. The use of the PtOEP sensitizer here was essential since the population of triplet states via intersystem crossing from excited singlet states in highly fluorescent BFA compounds was unlikely. In fact, no phosphorescence from the neat BFA films was detected under excitation at 337 nm at 5 K.

The sensitization enabled to create sufficient triplet population in BFA-Me and BFA-Ph compounds for detecting long-persisting phosphorescence at a 30 ms delay after the excitation pulse (Figure 3a). Triplet state energies of BFA-Me and BFA-Ph emitters, i.e., 1.71 eV (725 nm) and 1.69 eV (733 nm), respectively, were determined from the zeroth vibronic peaks of the phosporescence spectra and confirmed to lie well below that of the PtOEP sensitizer 1.92 eV (645 nm) (for PtOEP phosphorescence, see Figure 4). Such triplet energy order for the PtOEP-BFA pair ensured the sensitized TTA-UC scheme to be fully operational and capable of producing bright blue UC emission (Figure 3a,b).

Temperature Dynamics of TTA-UC. Temperature dependence of UC emission spectra in BFA/PtOEP films excited at the Q band of the sensitizer (532 nm) with a pulsed

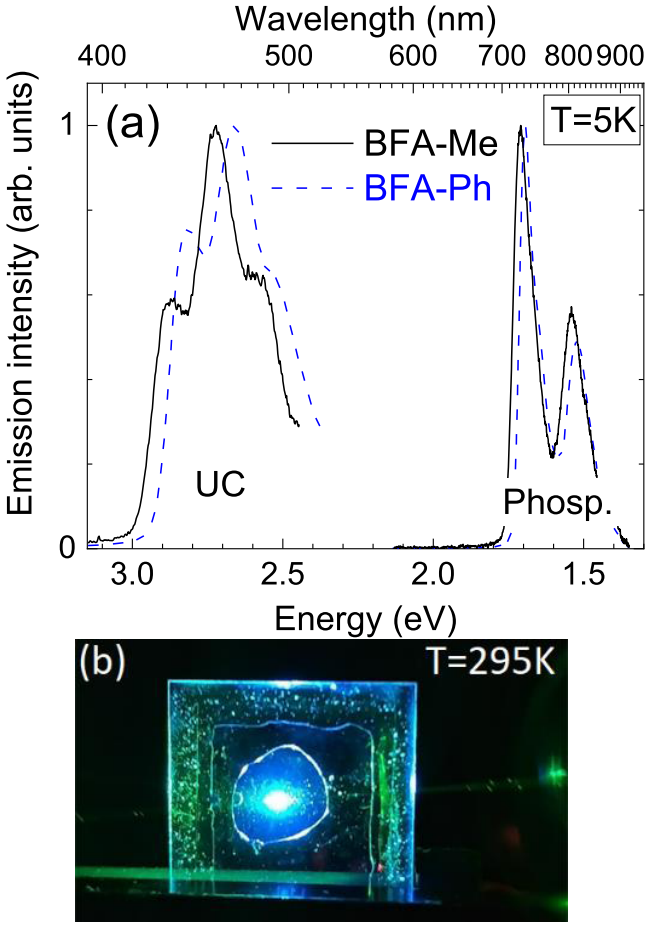

Figure 3. (a) UC emission (measured at a delay of 2 μs) and phosphorescence (measured at a delay of 30 ms) spectra of BFA/PtOEP films at 5 K. Excitation wavelength: 532 nm. (b) Picture of unfiltered green-to-blue upconversion in the BFA-Ph/PtOEP film obtained at room temperature under CW excitation at 532 nm.

Nd^{3+}:YAG laser is illustrated in Figure 4. The measured spectra were dominated by the UC emission peaking at ~460−480 nm as well as much weaker residual phosphorescence from the monodispersed PtOEP sensitizer at ~645 nm. We emphasize that in sharp contrast to matrix-free solid DPA/PtOEP systems reported previously,[45,46,48] UC intensity here is 10−100 times stronger than PtOEP phosphorescence, demonstrating the successful implementation of the structural modification of the emitter and optimization of PtOEP concentration (0.03 wt %) to attain amorphous BFA/PtOEP binary films with dramatically reduced exciton quenching, enhanced triplet transfer, and thus improved TTA-UC performance (as it will be shown below). Additional emission at ~780 nm observed in BFA-Me/PtOEP films was attributed to PtOEP aggregates (Figure 4a).[52,53] Surprisingly, the aggregation occurred at a very low sensitizer-to-emitter molar ratio of 1:3000, indicating limited miscibility of PtOEP in the BFA-Me host. We note that the spectral band due to PtOEP aggregates could not be discerned in the absorption spectra of BFA/PtOEP films (see Figure S9 in the Supporting Information and explanation therein), indicating that the number of aggregates is in turn very small as compared to that of the single PtOEP molecules. The only reason why PtOEP aggregates can be observed in the emission spectrum of the BFA-Me/PtOEP film is that the aggregate states are the lowest energy states. The triplet energy collection

https://dx.doi.org/10.1021/acs.jpcc.0c11048
J. Phys. Chem. C 2021, 125, 3764−3775

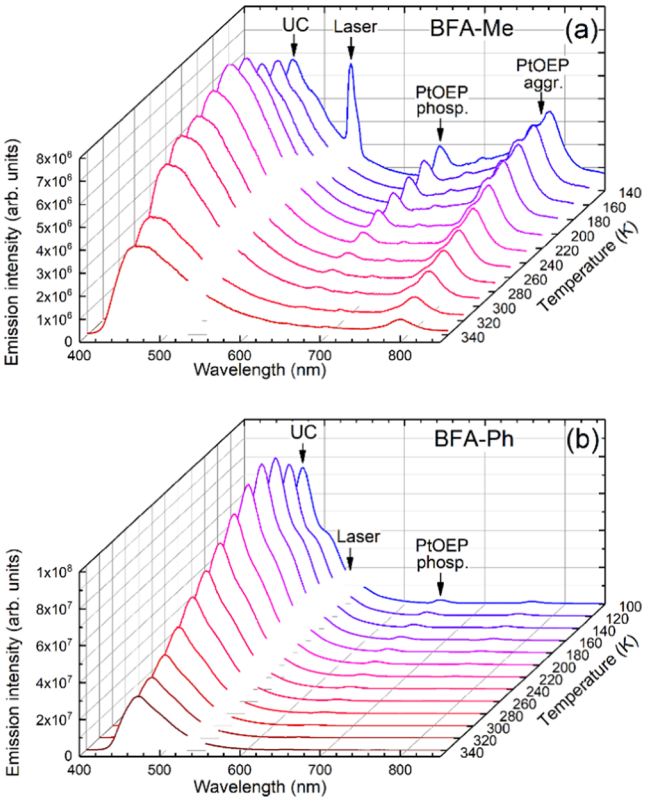

Figure 4. Emission spectra of (a) BFA-Me/PtOEP and (b) BFA-Ph/PtOEP films as a function of temperature, measured at a 10 μs delay after the excitation using 49 ms exposure. For clarity, the spectral region in the vicinity of the excitation wavelength (532 nm) was removed for BFA-Me/PtOEP films due to the residual signal of the incident light. Excitation energy density per pulse : 600 $\mu J \cdot cm^{-2}$.

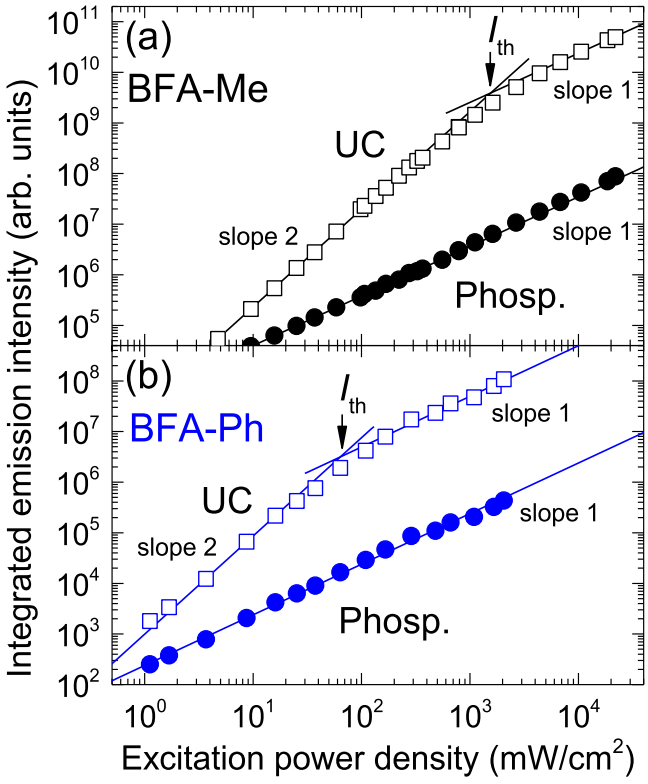

Figure 5. UC and PtOEP phosphorescence intensity as a function of the excitation power density of (a) BFA-Me/PtOEP and (b) BFA-Ph/PtOEP films. Excitation wavelength: 532 nm. The arrow indicates the threshold density, where the UC intensity switches from quadratic to linear regime.

to these states is driven by energy cascading down this pathway: [single PtOEP molecules (1.92 eV)] → [BFA-Me (1.71 eV)] → [PtOEP aggregates (1.59 eV)]. The emission due to aggregates, likely also accompanied by quenching in PtOEP dimers[45,46] contributed to the UC losses in BFA-Me/PtOEP films, as these were not utilized in the TTA-UC process. Conversely, the negligible PtOEP aggregate emission in the spectra of BFA-Ph/PtOEP films indicated that substitution of the methyl group by a phenyl group in the BFA emitter can resolve this issue, resulting in the homogeneous dispersion of the sensitizer, and consequently, virtually no associated UC losses (Figure 4b).

As a result, UC quantum yield values determined using the integrating sphere method[54] were found to be much higher for BFA-Ph/PtOEP films (Φ_{UC} = 3%) as compared to those for BFA-Me/PtOEP films (Φ_{UC} = 0.65%). We remind that the definition implies a maximum Φ_{UC} value of 50%. Φ_{UC} evaluation of the films was carried out at an excitation power density of 2 $W \cdot cm^{-2}$. Excitation at this level ensured a linear response of UC intensity versus power density for both films (Figure 5), thereby warranting domination of the TTA process over other possible decay pathways.[55,56] The onset (I_{th}) of the linear regime was found to be at substantially higher densities (I_{th} = 1.5 $W \cdot cm^{-2}$) for BFA-Me/PtOEP films as compared to that for BFA-Ph/PtOEP films (I_{th} = 0.06 $W \cdot cm^{-2}$). The much higher I_{th} in BFA-Me/PtOEP could be explained by the shorter triplet lifetime in BFA-Me (see Figure 7 and discussion below), a possibly smaller TTA rate, and additional energy losses due to PtOEP aggregation.

As expected, increasing temperature from the lowest up to the highest measured caused a decrease of PtOEP phosphorescence (Figure 4) in accordance with temperature-induced triplet state deactivation[57] and enhanced TET from PtOEP to BFA (Figure S10a in the Supporting Information). Phosphorescence intensity decayed monotonously with increasing temperature for both BFA/PtOEP films, as depicted in Figure S11 in the Supporting Information. Conversely, the temperature dependence of UC intensity varied in a non-monotonous manner, i.e., it increased up to its maximum value at temperatures (T_{max}) of 220 K and 160 K for BFA-Me/PtOEP and BFA-Ph/PtOEP films, respectively, and then steadily decreased above these temperatures. This intricate behavior of UC emission as a function of temperature is explicitly illustrated in Figure 6a. Since TTA-UC combines numerous processes of singlet and triplet origin, such UC dynamics could result from their complex interplay.

To discern the impact of triplet diffusion-facilitated processes on the UC temperature dynamics of BFA/PtOEP films, UC intensity variations with temperature were corrected for the influence of processes associated with singlets, namely, the changes in sensitizer absorption (Figure 6b) as well as changes in the FL intensity of the emitters BFA-Me and BFA-Ph (Figure 6c). We note that no intensity changes of absorption were observed for BFA-Me and BFA-Ph neat films in the temperature range studied. The corrected UC curves (Figure 6d) expressed a similar intensity increase with temperature up to T_{max}, yet roughly 2 times flattened slope

https://dx.doi.org/10.1021/acs.jpcc.0c11048
J. Phys. Chem. C 2021, 125, 3764−3775

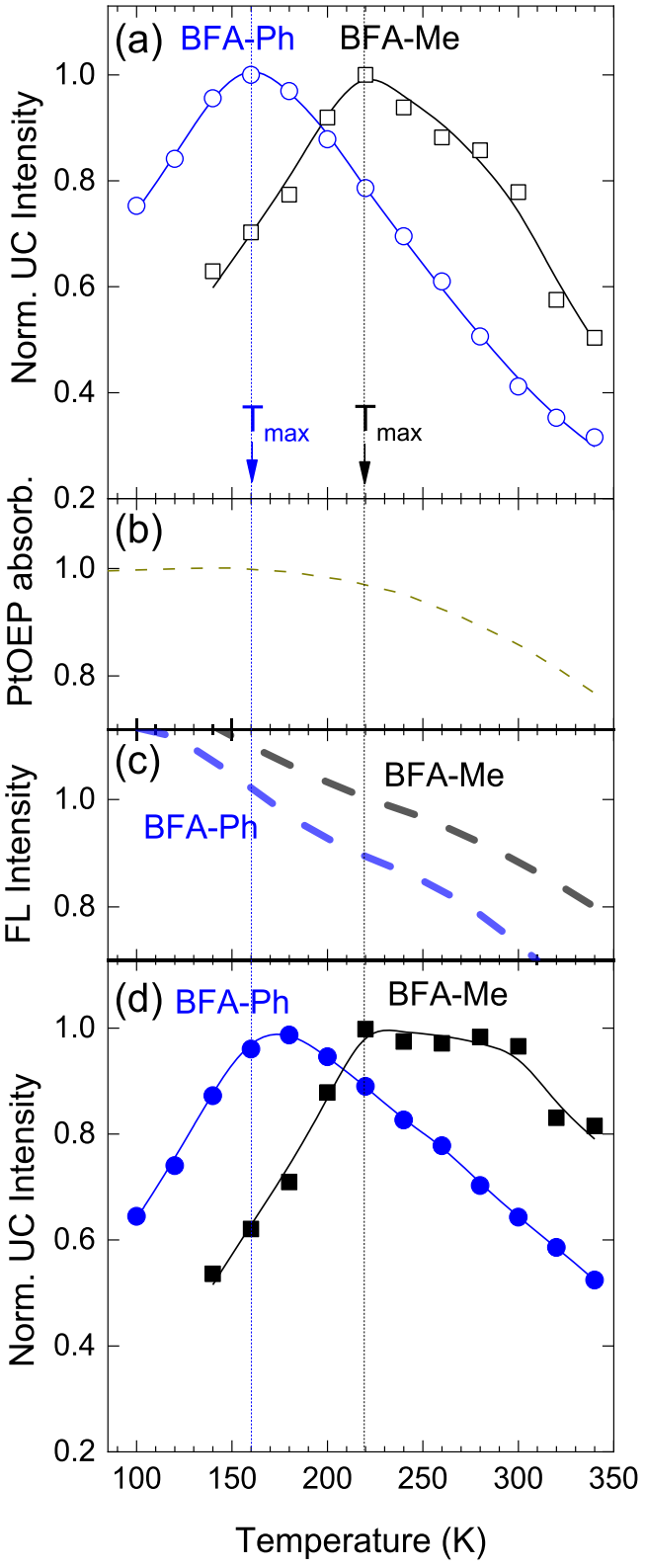

Figure 6. Normalized (a) UC intensity, (c) FL intensity of BFA/PtOEP films, and (b) PtOEP absorption as a function of temperature. (d) UC intensity of BFA/PtOEP films corrected for the temperature variations of PtOEP absorption and FL intensity of BFA represented in (b) and (c), respectively. The excitation wavelengths for UC and FL were 532 and 355 nm, respectively. Arrows mark temperatures at the maximal UC yields (T_{max}). Solid lines are guides to the eye.

above T_{max}, indicating a substantial portion of the singlet-related processes contributing to the temperature-dependent UC changes.

The initial UC intensity increase with temperature up to T_{max} could originate from the enhanced triplet transfer (TET) from PtOEP to BFA and/or improved triplet diffusion in BFA. Generally, the triplet diffusion, and thus TTA, is facilitated by thermally activated incoherent hopping of triplet excitons in disordered films. To determine whether the TET influences UC intensity behavior, we compared PtOEP phosphorescence intensity variations with temperature in the wide-band-gap host PMMA and low-gap hosts BFA-Me and BFA-Ph (Figure S10 in the Supporting Information). Since the triplet energy of PMMA (3.1 eV)[58] is well above that of PtOEP, TET from PtOEP is impossible and PtOEP phosphorescence decreases only due to temperature-induced triplet state deactivation to the ground state. Conversely, in the BFA films, TET from PtOEP to BFA is highly probable (the inset of Figure S10a), thereby giving rise to accelerated phosphorescence quenching of the sensitizer in these hosts. In fact, the phosphorescence was quenched by more than 3 orders of magnitude in both BFA hosts in the whole temperature range measured (100−350 K), implying TET efficiency in excess of (99.96 ± 0.02)% at all temperatures. The high TET efficiency at room temperature was also confirmed by phosphorescence lifetime quenching experiments of PtOEP in BFA films (Figure S12). Lifetimes were shortened from 109 μs (unquenched in PMMA) to 53−65 ns (quenched in BFA), indicating TET efficiencies in excess of (99.94 ± 0.05)% as evaluated from $\Phi_{TET} = 1 - \frac{\tau_{in\ BFA}}{\tau_{in\ PMMA}}$. The complete TET achieved already at low temperatures allowed to disregard its influence on the initial UC intensity rise with temperature and confirmed diffusion-assisted TTA to be responsible for this behavior (Figure 6d).

On the other hand, the continuous drop of UC intensity above T_{max}, which is quite remarkable, particularly for BFA-Ph/PtOEP (Figure 6d), is attributed to thermally activated triplet exciton diffusion followed by diffusion-facilitated exciton quenching at defect sites.[47,59,60] This implies that the optimal TTA-UC performance in the studied UC systems is achieved at temperatures much lower than the room temperature.

The dynamics of triplets and its impact on UC temperature behavior displayed in Figure 6d can be explained as follows. At relatively low temperatures, quenching sites are hardly accessible by the triplets due to their low diffusion lengths. However, the diffusion can still be sufficient (at an appropriately high triplet concentration) for promoting triplet encounter and thereby TTA-UC. The occurrence of T_{max} signifies a change of the regime from that governed by TTA to the one dominated by temperature-activated triplet quenching. Since both regimes result from incoherent hopping of excitons and are thermally activated, the T_{max} value depends on both the triplet diffusion and triplet quenching rate. Hence, as it was demonstrated for poly(*p*-phenylene) derivatives in ref 59, the higher triplet quenching rates (or higher defect concentration) will cause T_{max} to appear at lower temperatures provided the triplet diffusion of both films is similar. On the other hand, faster triplet diffusion will also imply lower T_{max} (as the triplets will be able to reach defect sites faster) given the triplet quenching rates are the same. Thus, the lower T_{max} in the BFA-Ph film as compared to the BFA-Me film could result from more profound triplet quenching or enhanced triplet

https://dx.doi.org/10.1021/acs.jpcc.0c11048
J. Phys. Chem. C 2021, 125, 3764−3775

exciton diffusion or both. To identify the dominant mechanism, UC emission transients serving as a probe of the triplet exciton lifetime were measured at different temperatures.

The transients obtained over the large temporal and intensity ranges for both BFA/PtOEP films are depicted in a log−log scale in Figure 7. We note that the excitation energy

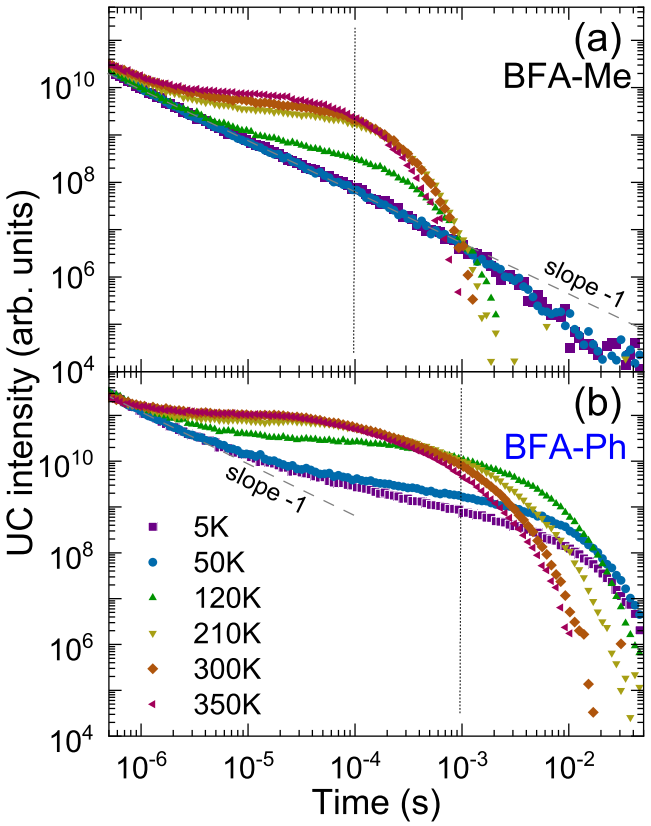

Figure 7. UC emission transients of (a) BFA-Me/PtOEP and (b) BFA-Ph/PtOEP films at different temperatures. The dotted line indicates the transition to the regime dominated by the spontaneous triplet decay. Excitation energy density per pulse: 600 $\mu J \cdot cm^{-2}$.

density (600 $\mu J \cdot cm^{-2}$ per pulse) employed for measuring the UC transients implies that just after the excitation, the triplet concentration is higher than that attained at I_{th} (for both BFA films), and thus at early times, the bimolecular recombination dominates over spontaneous emission. The detailed estimation of the triplet concentration is provided in the Supporting Information. The intensity of the UC emission depends on the product of the bimolecular rate constant for TTA—γ_{TTA}, with the square of the triplet concentration—$[T]$, i.e., $I(t) \propto \gamma_{TTA}(t) \cdot [T(t)]^2$.[61] Hence, initially, when the triplet concentration is quasistationary, the UC intensity reflects the time dependence of γ_{TTA}, while at later times, it reduces due to the spontaneous decay of the triplet states. From Figure 7, it is evident that this transition occurs at about 0.1 ms for BFA-Me, yet at 1 ms for BFA-Ph. Consequently, at the early stage, we observe a nearly constant intensity at high temperatures that gradually approaches a decay with a power law (slope of −1 on a log−log scale) as the temperature is reduced. Such decay dynamics were previously observed in numerous disordered films, like polyfluorenes, poly(*para*-phenylene vinylenes), etc.,[61−63] and attributed to the dispersive triplet exciton hopping over the randomly distributed density of states toward the energy minimum. The dynamics observed here in the initial time range matches perfectly with the predictions for $\gamma_{TTA}(t)$ obtained from Monte-Carlo simulations for a disordered density of states as a function of temperature.[64] As already mentioned, the decay at later times reflects the lifetime of the triplet states. Evidently, the lifetimes of BFA-Me are about 1 order of magnitude shorter than those of BFA-Ph. The extinction coefficients of both materials differ only a little (Figure S13 in the Supporting Information), hence the radiative rate of emission is also comparable and the reduced lifetime is a signature of a stronger nonradiative decay in BFA-Me.

A shorter lifetime in BFA-Me can result from either a faster intrinsic triplet decay or stronger triplet diffusivity and hence faster trapping and quenching at defect sites or from an increased concentration of triplet quenching sites. The intrinsic triplet decay in different BFA emitters was addressed by performing UC transient measurements of BFA-Me/PtOEP and BFA-Ph/PtOEP in a chloroform solution (see Figure S14 in the Supporting Information). The experiment allowed us to suppress the exciton diffusion-assisted quenching mechanism, while essentially leaving the intrinsic one. The estimated rather similar UC emission lifetimes (175 and 224 μs) of BFA emitters in solution could not account for the much larger difference in the lifetimes obtained for BFA films (Figure 7), thereby suggesting defect-related quenching to prevail. For a deeper insight into diffusion-assisted quenching, triplet exciton diffusion was quantitatively assessed in BFA-Me and BFA-Ph emitters.

Triplet Exciton Diffusion and Quenching. Triplet diffusivity in BFA/PtOEP films was determined using the time-resolved photoluminescence bulk-quenching technique.[49] In this technique, PCBM molecules are randomly dispersed in the BFA/PtOEP films at an increasing concentration to serve as triplet exciton quenchers.[65,66] By analyzing triplet lifetime quenching using a Stern−Volmer approach, we estimated the diffusion-controlled quenching efficiency and consequently evaluated the triplet diffusivity (D) and diffusion length (L_D). Owing to the nonemissive nature of the triplet excitons, their lifetime was probed by assessing the delayed UC signal from the singlet manifold generated via TTA.[21] Since the UC intensity scales as a square of the triplet concentration in an emitter, the triplet quenching efficiency (Q) can be expressed as

$$Q = 1 - \frac{\int \sqrt{UC_{PCBM}}\, dt}{\int \sqrt{UC_0}\, dt} \quad (1)$$

where UC_{PCBM} is UC transient (normalized at $t = 0$) with PCBM quenchers present, whereas UC_0 is an unquenched UC transient (normalized at $t = 0$). In fact, PCBM is known to quench both singlet and triplet excitons. However, since the singlets decay in the nanosecond time domain, while triplets (and subsequently UC signal emerging via TTA) in the millisecond time scale, PCBM-induced quenching will affect these decays in completely different time domains. Thus, the accelerated millisecond time-domain UC decay with increasing PCBM concentration, which is used for the estimation of triplet exciton diffusion, can occur only due to the triplet quenching. Singlet quenching in the millisecond time domain can manifest only through the lowered overall UC signal intensity, yet in no way can impact triplet lifetime and triplet

https://dx.doi.org/10.1021/acs.jpcc.0c11048
J. Phys. Chem. C 2021, 125, 3764−3775

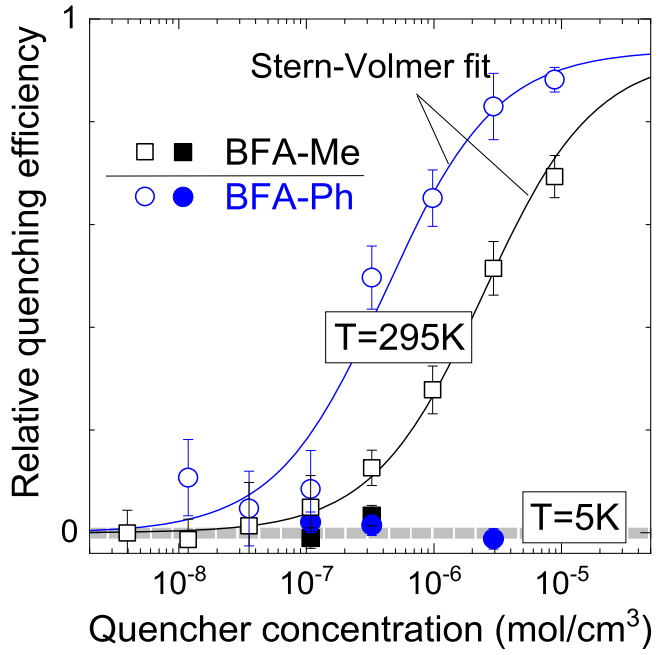

Figure 8. Relative quenching efficiency versus molar quencher concentration of BFA/PtOEP films at 5 and 295 K. Dashed gray line indicates zero quenching.

Table 1. Main Stern−Volmer Fitting Parameters at 295 K

	K_{SV} ($cm^3 \cdot mol^{-1}$)	f_a	r (nm)	D ($cm^2 \cdot s^{-1}$)	τ_{avg} (μs)	L_D (nm)
BFA-Me	$(4.1 \pm 0.22) \times 10^5$	0.94 ± 0.06	1.1 ± 0.04	$(1.18 \pm 0.13) \times 10^{-9}$	434 ± 42.2	17.5 ± 1.3
BFA-Ph	$(2.4 \pm 0.67) \times 10^6$	0.94 ± 0.06	1.1 ± 0.04	$(2.13 \pm 0.64) \times 10^{-9}$	1374 ± 153	41.9 ± 6.8

diffusion. Therefore, for the calculation of quenching efficiency according to eq 1, the integrals of UC transients normalized at $t = 0$ were used. UC transients of BFA/PtOEP films as a function of PCBM concentration at room temperature are shown in Figure S15; meanwhile, these and phosphorescence transients at 5 K are displayed in Figure S16 in the Supporting Information. The calculated triplet quenching efficiency (from the UC transients using eq 1) versus quencher concentration at 5 and 295 K is illustrated in Figure 8. The accelerated millisecond time-domain UC decay with increasing PCBM concentration observed at room temperature for both BFA/PtOEP films evidences thermally assisted triplet quenching. Conversely, at 5 K, PCBM content-independent UC and phosphorescence decay rates in the BFA/PtOEP films indicate suppression of triplet diffusion and diffusion-assisted quenching. This zero quenching efficiency at low temperatures is represented by the data points lying on the dashed gray line in Figure 8. To model Q behavior with respect to the quencher concentration (Q_c) at an elevated temperature, we exploited the "hindered access model" in combination with modified Stern−Volmer quenching analysis.[66] The model took into account the aggregation of the quencher at high concentrations, and in such a way enabled to quantitatively explain experimental results.

$$Q = f_a[1 - 1/(1 + K_{SV}Q_c)] \quad (2)$$

$$K_{SV} = 4\pi r P \tau N_A D \quad (3)$$

Here, f_a represents a fraction of emitter molecules accessible to the quencher, K_{SV} is the Stern−Volmer constant, r is the reactive radius (or the average distance between emitter molecules), P is the exciton quenching probability by the quencher (=1), N_A is Avogadro's number, and D is the diffusion constant. The experimental data were best described with $f_a = 0.94$; meanwhile, the slight deviation of the standard Stern−Volmer fits with $f_a = 1$ from the experimental data at the highest PCBM concentrations (see Figure S17 in the Supporting Information) suggested slight aggregation of PCBM.[66] The D derived from the fitting of experimental data displayed in Figure 8 using eqs 2 and 3 was utilized in the evaluation of L_D,

$$L_D = \sqrt{6D\tau} \quad (4)$$

where 6 is the dimensionality constant for three-dimensional (3D) diffusion.

The main parameters obtained from Stern−Volmer quenching analysis including the average triplet lifetime (τ_{avg}), triplet diffusion constant, and diffusion length are listed in Table 1. The comparison of these parameters indicates an almost twice as large triplet diffusivity in BFA-Ph as compared to that in BFA-Me, which accompanied by 3 times larger triplet decay time yields 2.5-fold longer triplet L_D in the amorphous BFA-Ph film. The larger triplet diffusivity at room temperature in the amorphous BFA-Ph films can be explained by a larger transfer integral due to the phenyl group at the 2-position of the anthracene core.

It is interesting to note that the obtained diffusion coefficients for the triplets in the matrix-free BFA films ($D \approx 10^{-9}$ $cm^2 \cdot s^{-1}$) are 1 order of magnitude lower than those obtained for DPA-doped PMMA films (at an emitter DPA content of ~30 wt % in the PMMA host).[21] We attribute lower D in the BFA films to the bulky peripheral dihexyl moieties of the BFA compounds, which act as certain intermolecular

https://dx.doi.org/10.1021/acs.jpcc.0c11048
J. Phys. Chem. C 2021, 125, 3764−3775

spacers ensuring amorphous morphology of the films; however, at a cost of a reduced triplet diffusion. The estimated triplet L_D in BFA films (18−42 nm) is consistent with the values typically obtained for neat amorphous films.[66−68]

In the context of Figure 7, we noted that the shorter lifetime of BFA-Me is either due to a higher triplet diffusivity or increased concentration of quenching sites. The obtained lower diffusivity in BFA-Me derived from Stern−Volmer analysis evidences a higher concentration of triplet quenching sites in BFA-Me as compared to BFA-Ph. The observation of emission related to PtOEP aggregates acting as additional (intrinsic) triplet quenchers in BFA-Me/PtOEP films (Figure 4a) supports this evidence. Considering that at room temperature, the quenching outcompetes TTA (see Figure 6d), the triplet L_D can be assumed to be limited by the average distance between the quenching sites. Taking into account that the room temperature L_D in BFA-Me and BFA-Ph differs by ∼2.4 times (Table 1), the difference in quenching site densities should amount to $(2.4)^3 \approx 14$ times.

Regardless of the 14 times lower density of quenching sites in BFA-Ph, the considerably enhanced diffusivity enables triplets to reach distant defect sites to cause UC quenching already at lower temperatures as compared to that of BFA-Me. The obtained results on high-emitter-content UC films are well in line with our previous work[27] and the work by Ogawa et al.,[69] which highlight the sensitivity of such films to impurities or defect sites, as they readily quench triplets and thereby severely deteriorates UC performance. Interestingly, suppression of defect-related quenching by confining triplets in UC dyes-containing liquid nanodroplets embedded within rigid polymers was recently demonstrated, which permitted to achieve Φ_{UC} comparable to that obtained in the best solution-based systems.[70]

Based on the data in Figure 6d, we can easily estimate that at room temperature, the quenchers reduce UC efficiency by a factor of ∼1.7 for the BFA-Ph/PtOEP film as compared to the maximal efficiency of this film achieved at T_{max} temperature. Thus, ultimately, in the absence of any triplet quenchers, i.e., in the hypothetical case of perfectly purified BFA-Ph material, we could expect at least a 1.7-fold enhancement of UC efficiency at room temperature, which would translate to room temperature Φ_{UC} values of 5.1% for the amorphous BFA-Ph/PtOEP film. Even though small-molecular-weight compounds can be purified to a higher degree with more ease than polymeric compounds, there will always be a remaining base level of trap sites. For example, Blom and co-workers identified a universal trap for electrons (and thus also excitons) at a trap concentration of 3×10^{17} cm^{-3}.[21,71] As it is not possible to remove all trap sites, a conceivable approach to shift the point of optimal UC efficiency, T_{max}, close to room temperature may also address tailoring the diffusivity. A reduced triplet diffusivity will suppress the access of the triplets to the quenching sites while still delivering sufficient TTA for UC.[60] This could, for example, be obtained by increasing the intermolecular distance through bulky non-conjugated side chains in the emitters. We note that for the studied BFA/PtOEP system, where triplet diffusion is rather moderate, the steric groups need to be chosen deliberately, i.e., not too bulky to avoid complete suppression of TTA at working temperatures, yet not very small as they will not prevent triplet quenching. Although the necessity to employ sterically demanding side groups to reduce exciton quenching was suggested previously,[45] an example of the solid BFA-Ph/PtOEP system points out that the triplet quenchers can be not only of intrinsic (caused by the aggregated emitter or sensitizer species) but also of extrinsic character (e.g., impurities).

CONCLUSIONS

In this work, by analyzing TTA-UC temperature dynamics, we were able to distinguish diffusion-facilitated triplet exciton quenching in the emitter species from other quenching processes in solid UC films and to show that it competes with TTA by reducing the triplet population. Although frequently overlooked, triplet quenching is demonstrated to be particularly relevant to high-emitter content UC films designed to promote triplet diffusivity. Herein, the issue was tackled in bicomponent matrix-free UC systems based on neat bisfluorene-anthracene (BFA) emitter films doped with a tiny amount of the PtOEP sensitizer (0.03 wt %) intended to prevent its aggregation as well as a singlet energy transfer from emitter back to the sensitizer. While the BFA/PtOEP films indeed expressed good triplet diffusivity in the range of 10^{-9} cm^2·s^{-1} at room temperature, the UC efficiency was found to be limited by the diffusion to the quenching sites. Although the density of nonradiative quenching sites in BFA-Ph was found to be lower (as evidenced by the prolonged UC lifetime) as compared to that of BFA-Me, the considerably enhanced diffusivity in BFA-Ph enabled triplets to reach distant defect sites to cause UC quenching already at lower temperatures. As a result, the maximum UC intensity was achieved well below room temperature, i.e., at 160 K for BFA-Ph and 220 K for BFA-Me. Our results suggest that high UC efficiencies at room temperature or above can be achieved not only by the obvious insight that defect levels need to be kept to a minimum by careful purification but, more importantly, by tailoring the triplet diffusivity such as to shift the maximum in the temperature-dependent UC efficiency to higher temperatures. The required reduction of triplet diffusivity may, for example, be obtained by increasing the intermolecular distance through suitable sterically demanding side groups.

ASSOCIATED CONTENT

Supporting Information

The Supporting Information is available free of charge at https://pubs.acs.org/doi/10.1021/acs.jpcc.0c11048.

Synthesis and identification; matrix assisted laser desorption ionization-time of flight mass (MALDI-TOF) spectra; differential scanning calorimetry scans; nanoscale thermal analysis of the BFA films; fluorescence spectra and transients of BFA dilute solutions and neat films; TTA-UC quantum yield of BFA/PtOEP films versus PtOEP concentration; absorption spectra of BFA/PtOEP films; PtOEP phosphorescence intensity and quantum yield versus temperature; PtOEP phosphorescence transients; absorption spectra of BFA in dilute solutions and neat films; UC emission transients in solution; UC emission transients as a function of PCBM quencher concentration at room temperature and 5 K; and estimation of the triplet concentration at excitation conditions used in UC transient measurements (PDF)

https://dx.doi.org/10.1021/acs.jpcc.0c11048
J. Phys. Chem. C 2021, 125, 3764−3775

AUTHOR INFORMATION

Corresponding Author

Karolis Kazlauskas − *Institute of Photonics and Nanotechnology, Vilnius University, LT-10257 Vilnius, Lithuania;* orcid.org/0000-0001-7900-0465; Email: karolis.kazlauskas@ff.vu.lt

Authors

Steponas Raišys − *Institute of Photonics and Nanotechnology, Vilnius University, LT-10257 Vilnius, Lithuania;* orcid.org/0000-0002-5810-7199

Ona Adomėnienė − *Institute of Photonics and Nanotechnology, Vilnius University, LT-10257 Vilnius, Lithuania*

Povilas Adomėnas − *Institute of Photonics and Nanotechnology, Vilnius University, LT-10257 Vilnius, Lithuania*

Alexander Rudnick − *Soft Matter Optoelectronics, Department of Physics & Bayreuth Institute of Macromolecular Research (BIMF), University of Bayreuth, 95440 Bayreuth, Germany*

Anna Köhler − *Soft Matter Optoelectronics, Department of Physics & Bayreuth Institute of Macromolecular Research (BIMF), University of Bayreuth, 95440 Bayreuth, Germany;* orcid.org/0000-0001-5029-4420

Complete contact information is available at: https://pubs.acs.org/10.1021/acs.jpcc.0c11048

Notes

The authors declare no competing financial interest.

ACKNOWLEDGMENTS

The research at Vilnius University was funded by a grant (No. S-MIP-17−77) from the Research Council of Lithuania (LMTLT). A.K. acknowledges support from the EU Marie-Skłodowska-Curie Action TADFlife and from the German Science Foundation (DFG) through GRK1640 ("Photophysics of Synthetic and Biological Multichromophoric Systems").

REFERENCES

(1) Khnayzer, R. S.; Blumhoff, J.; Harrington, J. A.; Haefele, A.; Deng, F.; Castellano, F. N. Upconversion-Powered Photoelectrochemistry. *Chem. Commun.* **2012**, *48*, 209−211.

(2) Kwon, O. S.; Song, H. S.; Conde, J.; Kim, H.; Artzi, N.; Kim, J.-H. Dual-Color Emissive Upconversion Nanocapsules for Differential Cancer Bioimaging In Vivo. *ACS Nano* **2016**, *10*, 1512−1521.

(3) Cheng, Y. Y.; Fückel, B.; MacQueen, R. W.; Khoury, T.; Clady, R. G. C. R.; Schulze, T. F.; Ekins-Daukes, N. J.; Crossley, M. J.; Stannowski, B.; Lips, K.; Schmidt, T. W. Improving the Light-Harvesting of Amorphous Silicon Solar Cells with Photochemical Upconversion. *Energy Environ. Sci.* **2012**, *5*, 6953−6959.

(4) Schulze, T. F.; Schmidt, T. W. Photochemical Upconversion: Present Status and Prospects for Its Application to Solar Energy Conversion. *Energy Environ. Sci.* **2015**, *8*, 103−125.

(5) Shang, Y.; Hao, S.; Yang, C.; Chen, G. Enhancing Solar Cell Efficiency Using Photon Upconversion Materials. *Nanomaterials* **2015**, *5*, 1782−1809.

(6) Singh-Rachford, T. N.; Castellano, F. N. Photon Upconversion Based on Sensitized Triplet−Triplet Annihilation. *Coord. Chem. Rev.* **2010**, *254*, 2560−2573.

(7) Zhao, J.; Ji, S.; Guo, H. Triplet−Triplet Annihilation Based Upconversion: From Triplet Sensitizers and Triplet Acceptors to Upconversion Quantum Yields. *RSC Adv.* **2011**, *1*, 937−950.

(8) Ye, C.; Wang, J.; Wang, X.; Ding, P.; Liang, Z.; Tao, X. A New Medium for Triplet−Triplet Annihilated Upconversion and Photocatalytic Application. *Phys. Chem. Chem. Phys.* **2016**, *18*, 3430−3437.

(9) Chandrasekaran, S.; Ngo, Y.-L. T.; Sui, L.; Kim, E. J.; Dang, D. K.; Chung, J. S.; Hur, S. H. Highly Enhanced Visible Light Water Splitting of CdS by Green to Blue Upconversion. *Dalton Trans.* **2017**, *46*, 13912−13919.

(10) Wang, W.; Liu, Q.; Zhan, C.; Barhoumi, A.; Yang, T.; Wylie, R. G.; Armstrong, P. A.; Kohane, D. S. Efficient Triplet−Triplet Annihilation-Based Upconversion for Nanoparticle Phototargeting. *Nano Lett.* **2015**, *15*, 6332−6338.

(11) Frazer, L.; Gallaher, J. K.; Schmidt, T. W. Optimizing the Efficiency of Solar Photon Upconversion. *ACS Energy Lett.* **2017**, *2*, 1346−1354.

(12) Borisov, S. M.; Larndorfer, C.; Klimant, I. Triplet−Triplet Annihilation-Based Anti-Stokes Oxygen Sensing Materials with a Very Broad Dynamic Range. *Adv. Funct. Mater.* **2012**, *22*, 4360−4368.

(13) Xu, M.; Zou, X.; Su, Q.; Yuan, W.; Cao, C.; Wang, Q.; Zhu, X.; Feng, W.; Li, F. Ratiometric Nanothermometer in Vivo Based on Triplet Sensitized Upconversion. *Nat. Commun.* **2018**, *9*, No. 2698.

(14) Huang, L.; Kakadiaris, E.; Vaneckova, T.; Huang, K.; Vaculovicova, M.; Han, G. Designing next Generation of Photon Upconversion: Recent Advances in Organic Triplet-Triplet Annihilation Upconversion Nanoparticles. *Biomaterials* **2019**, *201*, 77−86.

(15) Monguzzi, A.; Mauri, M.; Bianchi, A.; Dibbanti, M. K.; Simonutti, R.; Meinardi, F. Solid-State Sensitized Upconversion in Polyacrylate Elastomers. *J. Phys. Chem. C* **2016**, *120*, 2609−2614.

(16) Köhler, A.; Bässler, H. *Electronic Processes in Organic Semiconductors: An Introduction*; Wiley-VCH Verlag GmbH & Co. KGaA: Weinheim, Germany, 2015.

(17) Ogawa, T.; Yanai, N.; Monguzzi, A.; Kimizuka, N. Highly Efficient Photon Upconversion in Self-Assembled Light-Harvesting Molecular Systems. *Sci. Rep.* **2015**, *5*, No. 10882.

(18) Hoseinkhani, S.; Tubino, R.; Meinardi, F.; Monguzzi, A. Achieving the Photon Up-Conversion Thermodynamic Yield Upper Limit by Sensitized Triplet−Triplet Annihilation. *Phys. Chem. Chem. Phys.* **2015**, *17*, 4020−4024.

(19) Duan, P.; Yanai, N.; Kimizuka, N. Photon Upconverting Liquids: Matrix-Free Molecular Upconversion Systems Functioning in Air. *J. Am. Chem. Soc.* **2013**, *135*, 19056−19059.

(20) Zhou, Y.; Castellano, F. N.; Schmidt, T. W.; Hanson, K. On the Quantum Yield of Photon Upconversion via Triplet−Triplet Annihilation. *ACS Energy Lett.* **2020**, 2322−2326.

(21) Nicolai, H. T.; Kuik, M.; Wetzelaer, G. A. H.; de Boer, B.; Campbell, C.; Risko, C.; Brédas, J. L.; Blom, P. W. M. Unification of Trap-Limited Electron Transport in Semiconducting Polymers. *Nat. Mater.* **2012**, *11*, 882−887.

(22) Simon, Y. C.; Weder, C. Low-Power Photon Upconversion through Triplet−Triplet Annihilation in Polymers. *J. Mater. Chem.* **2012**, *22*, 20817−20830.

(23) Monguzzi, A.; Tubino, R.; Hoseinkhani, S.; Campione, M.; Meinardi, F. Low Power, Non-Coherent Sensitized Photon up-Conversion: Modelling and Perspectives. *Phys. Chem. Chem. Phys.* **2012**, *14*, 4322−4332.

(24) Merkel, P. B.; Dinnocenzo, J. P. Low-Power Green-to-Blue and Blue-to-UV Upconversion in Rigid Polymer Films. *J. Lumin.* **2009**, *129*, 303−306.

(25) Monguzzi, A.; Frigoli, M.; Larpent, C.; Tubino, R.; Meinardi, F. Low-Power-Photon Up-Conversion in Dual-Dye-Loaded Polymer Nanoparticles. *Adv. Funct. Mater.* **2012**, *22*, 139−143.

(26) Monguzzi, A.; Mauri, M.; Frigoli, M.; Pedrini, J.; Simonutti, R.; Larpent, C.; Vaccaro, G.; Sassi, M.; Meinardi, F. Unraveling Triplet Excitons Photophysics in Hyper-Cross-Linked Polymeric Nanoparticles: Toward the Next Generation of Solid-State Upconverting Materials. *J. Phys. Chem. Lett.* **2016**, *7*, 2779−2785.

(27) Raišys, S.; Kazlauskas, K.; Juršėnas, S.; Simon, Y. C. The Role of Triplet Exciton Diffusion in Light-Upconverting Polymer Glasses. *ACS Appl. Mater. Interfaces* **2016**, *8*, 15732−15740.

(28) Wu, M.; Congreve, D. N.; Wilson, M. W. B.; Jean, J.; Geva, N.; Welborn, M.; Van Voorhis, T.; Bulović, V.; Bawendi, M. G.; Baldo, M. A. Solid-State Infrared-to-Visible Upconversion Sensitized by Colloidal Nanocrystals. *Nat. Photonics* **2016**, *10*, 31−34.
(29) Turshatov, A.; Busko, D.; Kiseleva, N.; Grage; Stephan, L.; Howard, I. A.; Richards, B. S. Room-Temperature High-Efficiency Solid-State Triplet−Triplet Annihilation Up-Conversion in Amorphous Poly(Olefin Sulfone)s. *ACS Appl. Mater. Interfaces* **2017**, *9*, 8280−8286.
(30) Raišys, S.; Juršėnas, S.; Simon, Y. C.; Weder, C.; Kazlauskas, K. Enhancement of Triplet-Sensitized Upconversion in Rigid Polymers via Singlet Exciton Sink Approach. *Chem. Sci.* **2018**, *9*, 6796−6802.
(31) Gray, V.; Moth-Poulsen, K.; Albinsson, B.; Abrahamsson, M. Towards Efficient Solid-State Triplet−Triplet Annihilation Based Photon Upconversion: Supramolecular, Macromolecular and Self-Assembled Systems. *Coord. Chem. Rev.* **2018**, *362*, 54−71.
(32) Yanai, N.; Kimizuka, N. Recent Emergence of Photon Upconversion Based on Triplet Energy Migration in Molecular Assemblies. *Chem. Commun.* **2016**, *52*, 5354−5370.
(33) Kim, J.-H.; Deng, F.; Castellano, F. N.; Kim, J.-H. High Efficiency Low-Power Upconverting Soft Materials. *Chem. Mater.* **2012**, *24*, 2250−2252.
(34) Monguzzi, A.; Bianchi, F.; Bianchi, A.; Mauri, M.; Simonutti, R.; Ruffo, R.; Tubino, R.; Meinardi, F. High Efficiency Up-Converting Single Phase Elastomers for Photon Managing Applications. *Adv. Energy Mater.* **2013**, *3*, 680−686.
(35) Vadrucci, R.; Weder, C.; Simon, Y. C. Organogels for Low-Power Light Upconversion. *Mater. Horiz.* **2014**, *2*, 120−124.
(36) Duan, P.; Yanai, N.; Nagatomi, H.; Kimizuka, N. Photon Upconversion in Supramolecular Gel Matrixes: Spontaneous Accumulation of Light-Harvesting Donor−Acceptor Arrays in Nanofibers and Acquired Air Stability. *J. Am. Chem. Soc.* **2015**, *137*, 1887−1894.
(37) Vadrucci, R.; Monguzzi, A.; Saenz, F.; Wilts, B. D.; Simon, Y. C.; Weder, C. Nanodroplet-Containing Polymers for Efficient Low-Power Light Upconversion. *Adv. Mater.* **2017**, *29*, No. 1702992.
(38) Thévenaz, D. C.; Monguzzi, A.; Vanhecke, D.; Vadrucci, R.; Meinardi, F.; C. Simon, Y.; Weder, C. Thermoresponsive Low-Power Light Upconverting Polymer Nanoparticles. *Mater. Horiz.* **2016**, *3*, 602−607.
(39) Kang, J.-H.; Kim, S.-H.; Fernandez-Nieves, A.; Reichmanis, E. Amplified Photon Upconversion by Photonic Shell of Cholesteric Liquid Crystals. *J. Am. Chem. Soc.* **2017**, *139*, 5708−5711.
(40) Meinardi, F.; Ballabio, M.; Yanai, N.; Kimizuka, N.; Bianchi, A.; Mauri, M.; Simonutti, R.; Ronchi, A.; Campione, M.; Monguzzi, A. Quasi-Thresholdless Photon Upconversion in Metal−Organic Framework Nanocrystals. *Nano Lett.* **2019**, *19*, 2169−2177.
(41) Ogawa, T.; Hosoyamada, M.; Yurash, B.; Nguyen, T.-Q.; Yanai, N.; Kimizuka, N. Donor−Acceptor−Collector Ternary Crystalline Films for Efficient Solid-State Photon Upconversion. *J. Am. Chem. Soc.* **2018**, *140*, 8788−8796.
(42) Reghu, R. R.; Simokaitiene, J.; Grazulevicius, J. V.; Raisys, S.; Kazlauskas, K.; Jursenas, S.; Jankauskas, V.; Reina, A. Synthesis and Properties of Hole-Transporting Triphenylamine-Derived Dendritic Compounds. *Dyes Pigm.* **2015**, *115*, 135−142.
(43) Vadrucci, R.; Weder, C.; Simon, Y. C. Low-Power Photon Upconversion in Organic Glasses. *J. Mater. Chem. C* **2014**, *2*, 2837−2841.
(44) Ogawa, T.; Yanai, N.; Kouno, H.; Kimizuka, N. Kinetically Controlled Crystal Growth Approach to Enhance Triplet Energy Migration-Based Photon Upconversion. *J. Photonics Energy* **2017**, *8*, No. 022003.
(45) Goudarzi, H.; Keivanidis, P. E. Triplet−Triplet Annihilation-Induced Up-Converted Delayed Luminescence in Solid-State Organic Composites: Monitoring Low-Energy Photon Up-Conversion at Low Temperatures. *J. Phys. Chem. C* **2014**, *118*, 14256−14265.
(46) Goudarzi, H.; Keivanidis, P. E. All-Solution-Based Aggregation Control in Solid-State Photon Upconverting Organic Model Composites. *ACS Appl. Mater. Interfaces* **2017**, *9*, 845−857.
(47) Goudarzi, H.; Limbu, S.; Cabanillas-González, J.; Zenonos, V. M.; Kim, J.-S.; Keivanidis, P. E. Impact of Molecular Conformation on Triplet-Fusion Induced Photon Energy up-Conversion in the Absence of Exothermic Triplet Energy Transfer. *J. Mater. Chem. C* **2019**, *7*, 3634−3643.
(48) Karpicz, R.; Puzinas, S.; Gulbinas, V.; Vakhnin, A.; Kadashchuk, A.; Rand, B. P. Exciton Dynamics in an Energy Up-Converting Solid State System Based on Diphenylanthracene Doped with Platinum Octaethylporphyrin. *Chem. Phys.* **2014**, *429*, 57−62.
(49) Lin, J. D. A.; Mikhnenko, O. V.; Chen, J.; Masri, Z.; Ruseckas, A.; Mikhailovsky, A.; Raab, R. P.; Liu, J.; Blom, P. W. M.; Loi, M. A.; et al. Systematic Study of Exciton Diffusion Length in Organic Semiconductors by Six Experimental Methods. *Mater. Horiz.* **2014**, *1*, 280−285.
(50) Laquai, F.; Wegner, G.; Im, C.; Büsing, A.; Heun, S. Efficient Upconversion Fluorescence in a Blue-Emitting Spirobifluorene-Anthracene Copolymer Doped with Low Concentrations of Pt(II)-Octaethylporphyrin. *J. Chem. Phys.* **2005**, *123*, No. 074902.
(51) Kondakov, D. Y.; Pawlik, T. D.; Hatwar, T. K.; Spindler, J. P. Triplet Annihilation Exceeding Spin Statistical Limit in Highly Efficient Fluorescent Organic Light-Emitting Diodes. *J. Appl. Phys.* **2009**, *106*, No. 124510.
(52) Kalinowski, J.; Stampor, W.; Szmytkowski, J.; Cocchi, M.; Virgili, D.; Fattori, V.; Di Marco, P. Photophysics of an Electrophosphorescent Platinum (II) Porphyrin in Solid Films. *J. Chem. Phys.* **2005**, *122*, No. 154710.
(53) Bansal, A. K.; Holzer, W.; Penzkofer, A.; Tsuboi, T. Absorption and Emission Spectroscopic Characterization of Platinum-Octaethyl-Porphyrin (PtOEP). *Chem. Phys.* **2006**, *330*, 118−129.
(54) de Mello, J. C.; Wittmann, H. F.; Friend, R. H. An Improved Experimental Determination of External Photoluminescence Quantum Efficiency. *Adv. Mater.* **1997**, *9*, 230−232.
(55) Monguzzi, A.; Mezyk, J.; Scotognella, F.; Tubino, R.; Meinardi, F. Upconversion-Induced Fluorescence in Multicomponent Systems: Steady-State Excitation Power Threshold. *Phys. Rev. B* **2008**, *78*, No. 195112.
(56) Haefele, A.; Blumhoff, J.; Khnayzer, R. S.; Castellano, F. N. Getting to the (Square) Root of the Problem: How to Make Noncoherent Pumped Upconversion Linear. *J. Phys. Chem. Lett.* **2012**, *3*, 299−303.
(57) Ribierre, J. C.; Ruseckas, A.; Samuel, I. D. W.; Staton, S. V.; Burn, P. L. Temperature Dependence of the Triplet Diffusion and Quenching Rates in Films of an Ir (Ppy) 3-Cored Dendrimer. *Phys. Rev. B* **2008**, *77*, No. 085211.
(58) Avdeenko, A. A.; Dobrovolskaya, T. L.; Kultchitsky, V. A.; Naboikin, Y. V.; Pakulov, S. N. Temperature Dependence of Luminescence Decay Time of Benzyl. *J. Lumin.* **1976**, *11*, 331−337.
(59) Hoffmann, S. T.; Koenen, J.-M.; Scherf, U.; Bauer, I.; Strohriegl, P.; Bässler, H.; Köhler, A. Triplet−Triplet Annihilation in a Series of Poly(p-Phenylene) Derivatives. *J. Phys. Chem. B* **2011**, *115*, 8417−8423.
(60) Saxena, R.; Meier, T.; Athanasopoulos, S.; Bässler, H.; Köhler, A. Kinetic Monte Carlo Study of Triplet-Triplet Annihilation in Conjugated Luminescent Materials. *Phys. Rev. Appl.* **2020**, *14*, No. 034050.
(61) Hertel, D.; Bässler, H.; Guentner, R.; Scherf, U. Triplet-Triplet Annihilation in a Poly(Fluorene)-Derivative. *J. Chem. Phys.* **2001**, *115*, 10007−10013.
(62) Rothe, C.; Monkman, A. P. Triplet Exciton Migration in a Conjugated Polyfluorene. *Phys. Rev. B* **2003**, *68*, No. 075208.
(63) Jankus, V.; Snedden, E. W.; Bright, D. W.; Whittle, V. L.; Williams, J. A. G.; Monkman, A. Energy Upconversion via Triplet Fusion in Super Yellow PPV Films Doped with Palladium Tetraphenyltetrabenzoporphyrin: A Comprehensive Investigation of Exciton Dynamics. *Adv. Funct. Mater.* **2013**, *23*, 384−393.
(64) Scheidler, M.; Cleve, B.; Bässler, H.; Thomas, P. Monte Carlo Simulation of Bimolecular Exciton Annihilation in an Energetically Random Hopping System. *Chem. Phys. Lett.* **1994**, *225*, 431−436.

https://dx.doi.org/10.1021/acs.jpcc.0c11048
J. Phys. Chem. C 2021, 125, 3764−3775

(65) Schlenker, C. W.; Chen, K.-S.; Yip, H.-L.; Li, C.-Z.; Bradshaw, L. R.; Ochsenbein, S. T.; Ding, F.; Li, X. S.; Gamelin, D. R.; Jen, A. K.-Y.; Ginger, D. S. Polymer Triplet Energy Levels Need Not Limit Photocurrent Collection in Organic Solar Cells. *J. Am. Chem. Soc.* **2012**, *134*, 19661−19668.
(66) Hsu, H.-Y.; Vella, J. H.; Myers, J. D.; Xue, J.; Schanze, K. S. Triplet Exciton Diffusion in Platinum Polyyne Films. *J. Phys. Chem. C* **2014**, *118*, 24282−24289.
(67) Schwartz, G.; Reineke, S.; Rosenow, T. C.; Walzer, K.; Leo, K. Triplet Harvesting in Hybrid White Organic Light-Emitting Diodes. *Adv. Funct. Mater.* **2009**, *19*, 1319−1333.
(68) Rand, B. P.; Schols, S.; Cheyns, D.; Gommans, H.; Girotto, C.; Genoe, J.; Heremans, P.; Poortmans, J. Organic Solar Cells with Sensitized Phosphorescent Absorbing Layers. *Org. Electron.* **2009**, *10*, 1015−1019.
(69) Ogawa, T.; Yanai, N.; Fujiwara, S.; Nguyen, T.-Q.; Kimizuka, N. Aggregation-Free Sensitizer Dispersion in Rigid Ionic Crystals for Efficient Solid-State Photon Upconversion and Demonstration of Defect Effects. *J. Mater. Chem. C* **2018**, *6*, 5609−5615.
(70) Saenz, F.; Ronchi, A.; Mauri, M.; Vadrucci, R.; Meinardi, F.; Monguzzi, A.; Weder, C. Nanostructured Polymers Enable Stable and Efficient Low-Power Photon Upconversion. *Adv. Funct. Mater.* **2020**, No. 2004495.
(71) Mikhnenko, O. V.; Blom, P. W. M.; Nguyen, T.-Q. Exciton Diffusion in Organic Semiconductors. *Energy Environ. Sci.* **2015**, *8*, 1867−1888.

https://dx.doi.org/10.1021/acs.jpcc.0c11048
J. Phys. Chem. C 2021, 125, 3764−3775